

Crystal and Electronic Structures of One-Dimensional Transition Metal Thiophosphates: ANb_2PS_{10} ($A=Na, Ag$)

Eun-Young Goh,^{*} Sung-Jin Kim,^{*,1} and Dongwoon Jung^{†,1}

^{*}Department of Chemistry, Ewha Womans University, #120-750, Seoul, South Korea; and [†]Department of Chemistry, Wonkwang University, Iksan, Jeonbuk, #570-749, South Korea

Received January 23, 2002; in revised form May 30, 2002; accepted July 15, 2002

A new quaternary compound $NaNb_2PS_{10}$ was prepared by reacting the mixture of Nb, P_2S_5 , S and Na_2S at $750^\circ C$. $AgNb_2PS_{10}$ was also synthesized by the direct solid-state reaction of Ag, Nb, P and S at $900^\circ C$. Their structures were determined by single-crystal X-ray diffraction method. The needle-shape crystals of the two compounds crystallize in the common monoclinic space group $C2/c$. $NaNb_2PS_{10}$ crystallizes into purple crystals with cell dimensions of $a = 24.7634(10) \text{ \AA}$, $b = 7.8407(11) \text{ \AA}$, $c = 12.947(3) \text{ \AA}$, $\beta = 90.83(2)^\circ$ and $Z = 8$. $AgNb_2PS_{10}$ had dark-gray crystals with cell dimensions of $a = 23.9609(10) \text{ \AA}$, $b = 7.7692(11) \text{ \AA}$, $c = 12.910(3) \text{ \AA}$, $\beta = 94.49(2)^\circ$ and $Z = 8$. These structures consist of one-dimensional infinite chains built by $[Nb_2S_{12}]$ and $[PS_4]$ units. The Nb atoms are centered in distorted bicapped trigonal prismatic polyhedra and the neighboring polyhedra share square faces and edges to make Nb–Nb pairs. $[PS_4]$ units are tetrahedra composed of one S atom at the prism corner and two other capping S atoms and an additional S atom. Ag^+ and Na^+ cations in $NaNb_2PS_{10}$ and $AgNb_2PS_{10}$ reside in the van der Waals gap of sulfur atoms between infinite chains. Calculation of the electronic structure shows that the two compounds are semiconducting materials. Optically measured band gaps were 1.72 and 1.77 eV for $NaNb_2PS_{10}$ and $AgNb_2PS_{10}$, respectively. © 2002 Elsevier Science (USA)

Key Words: thiophosphates; low-dimensional structures; –S–S– bridges; intercalated compounds; electron transfer.

INTRODUCTION

Transition metal thiophosphates have been actively investigated due to their structural low dimensionality and importance as oxidizing host materials for secondary lithium batteries (1). Well-known examples of transition metal thiophosphates include layered MPS_3 (Mn, Fe, Cd, Co, Ni, Zn) (2), and mixed metal derivatives $MM'P_2S_6$ ($M,$

$M' = Ag, Cr; Ag, In$) (3), in which the ethane-like P_2S_6 unit is the common building block. Early transition-metal thiophosphates with various phosphorus–sulfur polyanions $[P_nQ_m]^{x-}$ and low-dimensional structures have been reported. For example, V_2PS_{10} is one-dimensional (4), $VP_{0.2}S_2$, $VP_{0.17}S_2$, $V_2P_4S_{13}$, Nb_2PS_{10} , $Nb_4P_2S_{21}$ and NbP_2S_8 are two-dimensional compounds possessing the PS_4^{3-} unit (5–9). To understand how the low-dimensional thiophosphates can be applied to the matrix materials for secondary lithium batteries, it is necessary to synthesize the cation intercalated compounds and to analyze their electronic structures. KNb_2PS_{10} is the first known alkali metal contained compound (10) whose structure is closely related to that of Nb_2PS_{10} and $Nb_4P_2S_{21}$. As already known, Nb_2PS_{10} and $Nb_4P_2S_{21}$ are two-dimensional compounds because of the –S–S– or –S–S–S– bridges between the one-dimensional chains. However, the –S–S– bridges are broken when K^+ ions are filled between chains thereafter forming one-dimensional KNb_2PS_{10} . Recently, we synthesized more family members of one-dimensional quaternary thiophosphates, ANb_2PS_{10} ($A = Na, Ag$), whose structures are also related to those of 2D- Nb_2PS_{10} and 2D- $Nb_4P_2S_{21}$. Electron transfer from cation to one-dimensional matrix becomes an interesting area to be investigated hereafter. Previous band structure investigated on the ternary thiophosphates M_2PS_{10} ($M = Nb, V$) suggests that the empty or partially filled d -block orbitals of transition metals are responsible for the lithium intercalation (11). Since not many examples of alkali metal contained Nb_2PS_{10} -related compounds are structurally characterized, the effects of bonding and electronic structural change upon intercalation have not been completely understood. Since there are some structural changes between M_2PS_{10} and ANb_2PS_{10} ($A =$ alkali metals), the prediction of the electron structure of ANb_2PS_{10} based on the layered M_2PS_{10} might be incorrect. Herein, we present the synthesis, structural and electronic characterization of new quaternary phases ANb_2PS_{10}

¹To whom correspondence should be addressed. Fax: +82-2-3277-2384. E-mail: sjkim@ewha.ac.kr.



($A = \text{Na}, \text{Ag}$). The structural differences between $\text{KNb}_2\text{PS}_{10}$ and $\text{ANb}_2\text{PS}_{10}$ ($A = \text{Na}, \text{Ag}$) are discussed.

EXPERIMENTAL SECTION

Synthesis

$\text{NaNb}_2\text{PS}_{10}$ was prepared from a mixture of Na_2S (Dukan), Nb powder (Kojundo 99.9%), P_2S_5 (Fluka > 98%) and S powder (Aldrich 99.999%) in a molar ratio of 0.93:1:3:4, where Na_2S was used as a flux as well as a starting material. $\text{AgNb}_2\text{PS}_{10}$ was prepared from the stoichiometric quantities of Ag powder (Kojima 99.99%), Nb powder, P powder (Aldrich 99.99%) and S powder in a molar ratio of 1:2:1:10. The reacting mixture with a total mass of ~ 1 g was double-sealed in an evacuated quartz tube and heated at 750°C for 6 days for $\text{NaNb}_2\text{PS}_{10}$ and 900°C for 2 weeks for $\text{AgNb}_2\text{PS}_{10}$. Then, to obtain single crystals with a suitable size for structural determination, the heated products were slowly cooled to room temperature ($2^\circ\text{C}/\text{h}$).

The reactions lead to the formation of purple needle crystals for $\text{NaNb}_2\text{PS}_{10}$, and shiny dark-gray needle crystals for $\text{AgNb}_2\text{PS}_{10}$. The two compounds were stable in air and in moisture. From the reaction product for $\text{NaNb}_2\text{PS}_{10}$, unreacted excess Na_2S flux was observed at the hot end and some yellowish by-products at the cold end. Ternary NbP_2S_8 compounds were detected as a minor phase in the reaction for $\text{NaNb}_2\text{PS}_{10}$. The product was washed with DMF, ethanol and distilled water several times to remove the flux and by-products. Once the stoichiometry was determined from the X-ray single-crystal structure analysis, $\text{NaNb}_2\text{PS}_{10}$ was prepared rationally as a single phase starting from the exact stoichiometric ratio. Any observable evidence of side products of ternary or quaternary phases was not detected in the reaction for $\text{AgNb}_2\text{PS}_{10}$. The chemical compositions of the crystals were confirmed by an energy-dispersive X-ray (EDX) spectrometer equipped with an electron probe microanalysis (EPMA; JXA-9600, EDX; LinkeXL) for both compounds. Incorporation of Si from the quartz tube was not detected in either phase.

Structural Analysis

Preliminary examination and data collection were performed with $\text{MoK}_{\alpha 1}$ radiation ($\lambda = 0.71073 \text{ \AA}$) on an Enraf Nonius diffractometer equipped with an incident beam monochromator graphite crystal. The unit cell parameters and an orientation matrix for data collection were obtained from the least-squares refinement, using the setting angles of 25 reflections in the range of $22^\circ < 2\theta < 29^\circ$. The observed Laue symmetry and systematic extinctions ($h00, h = 2n + 1; 0k0, k = 2n + 1; 00l$ and

$h0l, l = 2n + 1; hk0, h + k = 2n + 1$) for the two compounds were indicative of the space groups $C_{2h}^6 - C2/c$ and $C_s^4 - Cc$. The centrosymmetric $C2/c$ was assumed and subsequent refinements confirmed the choice of this space group for the two compounds.

Intensity data were collected with the $\omega-2\theta$ scan technique. The intensities of three standard reflections measured every hour showed no significant deviations during the data collection. The initial positions of all atoms were obtained from the direct methods of the SHELXS-86 program (12). The structure was refined by full-matrix least-squares techniques using the SHELXL-93 program (13). The final cycle of refinement performed on F_o^2 with 2218 unique reflections converged to residuals wR_2 ($F_o^2 > 0$) = 0.1394 and the conventional R index based on the reflections having $F_o^2 > 2\sigma$ (F_o^2) was 0.0495 for $\text{NaNb}_2\text{PS}_{10}$. The final refinement of 2097 unique reflections gave wR_2 ($F_o^2 > 0$) = 0.1400 and the conventional R index based on the reflections having $F_o^2 > 2\sigma$ (F_o^2) was 0.0447 for $\text{AgNb}_2\text{PS}_{10}$.

Crystallographic data for $\text{NaNb}_2\text{PS}_{10}$ and $\text{AgNb}_2\text{PS}_{10}$ are given in Table 1. Tables 2 and 3 list final fractional atomic coordinates and displacement parameters for $\text{NaNb}_2\text{PS}_{10}$ and $\text{AgNb}_2\text{PS}_{10}$. Selected bond distances and angles for $\text{NaNb}_2\text{PS}_{10}$ and $\text{AgNb}_2\text{PS}_{10}$ are listed in Table 4.

Electronic Structure Calculation

Electronic structure calculations were performed by the extended Hückel method within the framework of tight-binding approximation (14(a)). Density of states (DOS) and crystal orbital overlap populations (COOP) were calculated based on the given crystal structure. The atomic orbital parameters employed in the calculation were the default values in the CAESAR program (14(b)), which are listed in Table 5.

TABLE 1
Crystallographic Data for $\text{NaNb}_2\text{PS}_{10}$ and $\text{AgNb}_2\text{PS}_{10}$

Empirical formula	$\text{NaNb}_2\text{PS}_{10}$	$\text{AgNb}_2\text{PS}_{10}$
Formula weight (g mol^{-1})	560.38	645.26
Temperature (K)	293(2)	293(2)
Wavelength (\AA)	0.71073	0.71073
Crystal system	Monoclinic	Monoclinic
Space group	$C_{2h}^6 - C2/c$	$C_{2h}^6 - C2/c$
Unit cell dimensions (\AA)	$a = 24.7634(10)$ $b = 7.8407(11)$ $c = 12.947(3)$ $\beta = 90.83(2)^\circ$	$a = 23.9609(10)$ $b = 7.7692(11)$ $c = 12.910(3)$ $\beta = 94.49(2)^\circ$
Volume (\AA^3)	2513.7(7)	2396.0(7)
Z	8	8
Density (calculated) (g cm^{-3})	2.962	3.578
$R_1(F_o^2 > 2\sigma(F_o^2))$	0.0495	0.0447
$wR_2(F_o^2 > 0)$	0.1394	0.1400

TABLE 2
Atomic Coordinates and Equivalent Isotropic Displacement Factors $U_{\text{(eq)}} (\text{\AA}^2)$ for $\text{NaNb}_2\text{PS}_{10}$

Atom	<i>x</i>	<i>y</i>	<i>z</i>	$U_{\text{(eq)}}^a$
Na1	0.4431(1)	0.4969(5)	0.3806(3)	0.039(1)
Nb1	0.3582(1)	0.0661(1)	0.2769(1)	0.015(1)
Nb2	0.3579(1)	0.9398(1)	0.4867(1)	0.015(1)
P1	0.3955(1)	0.3927(2)	0.1293(1)	0.018(1)
S1	0.4290(1)	0.1508(2)	0.1332(1)	0.017(1)
S2	0.4306(1)	0.1222(2)	0.4188(1)	0.022(1)
S3	0.2882(1)	0.0497(2)	0.1297(1)	0.018(1)
S4	0.3499(1)	0.3937(2)	0.2604(1)	0.021(1)
S5	0.4316(1)	0.8869(2)	0.3512(1)	0.022(1)
S6	0.3491(1)	0.6122(2)	0.4974(1)	0.022(1)
S7	0.3414(1)	0.8488(2)	0.1333(1)	0.019(1)
S8	0.2871(1)	0.1285(2)	0.4041(1)	0.023(1)
S9	0.2868(1)	0.8837(3)	0.3561(1)	0.024(1)
S10	0.4475(1)	0.5858(2)	0.1287(2)	0.030(1)

^a $U_{\text{(eq)}}$ is defined as one-third of the trace of the orthogonalized U_{ij} tensor.

TABLE 4
Selected Bond Distances (\AA) and Bond Angles (deg) for $\text{NaNb}_2\text{PS}_{10}$ and $\text{AgNb}_2\text{PS}_{10}$

	$\text{NaNb}_2\text{PS}_{10}$	$\text{AgNb}_2\text{PS}_{10}$		$\text{NaNb}_2\text{PS}_{10}$	$\text{AgNb}_2\text{PS}_{10}$
Nb1–S8	2.478(2)	2.462(3)	Nb1–S3	2.562(2)	2.539(3)
Nb1–S5	2.480(2)	2.515(3)	Nb1–S4	2.585(2)	2.571(3)
Nb1–S9	2.507(2)	2.545(3)	Nb1–S2	2.585(2)	2.455(3)
Nb1–S7	2.552(2)	2.547(3)	Nb1–S1	2.659(2)	2.656(3)
Nb2–S9	2.464(2)	2.469(3)	Nb2–S7	2.558(2)	2.546(3)
Nb2–S2	2.470(2)	2.499(3)	Nb2–S6	2.581(2)	2.625(3)
Nb2–S8	2.521(2)	2.553(3)	Nb2–S5	2.582(2)	2.474(3)
Nb2–S3	2.552(2)	2.564(3)	Nb2–S1	2.666(2)	2.649(3)
Nb1–Nb2	2.891(1)	2.870(2)	Nb1–Nb2	3.757(1)	3.756(2)
P–S10	1.988(3)	1.987(5)	P–S4	2.051(2)	2.048(4)
P–S6	2.045(2)	2.057(4)	P–S1	2.071(3)	2.064(4)
S2–S5	2.042(3)	2.022(5)	S3–S7	2.053(2)	2.056(4)
S8–S9	2.017(3)	2.046(5)			
S10–P–S6	111.57(11)	112.5(2)	S10–P–S1	115.96(11)	118.0(2)
S10–P–S4	111.39(11)	109.3(2)	S6–P–S1	102.89(10)	101.2(2)
S6–P–S4	112.44(11)	111.5(2)	S4–P–S1	102.05(10)	103.9(2)

Solid-State UV/Vis Spectroscopy

Measurements of optical diffuse reflectance were performed at room temperature with Shimadzu UV-3101PC double-beam, double-monochromator spectrophotometer. BaSO_4 was used as a 100% reflectance standard. Samples were prepared by grinding them to a fine powder and spreading them on the compacted surface of the standard material preloaded into a sample holder. The reflectances vs wavelength data were converted to absorption data through the Kubelka–Munk function (15).

TABLE 3
Atomic Coordinates and Equivalent Isotropic Displacement Factors $U_{\text{(eq)}} (\text{\AA}^2)$ for $\text{AgNb}_2\text{PS}_{10}$

Atom	<i>x</i>	<i>y</i>	<i>z</i>	$U_{\text{(eq)}}^a$
Ag1	0.0557(1)	0.5129(2)	0.0995(1)	0.041(1)
Nb1	0.1393(1)	0.0550(1)	0.0043(1)	0.011(1)
Nb2	0.1378(1)	0.9303(1)	0.2133(1)	0.011(1)
P1	0.0970(1)	0.3917(4)	0.8631(2)	0.016(1)
S1	0.0650(1)	0.1453(4)	0.8505(2)	0.013(1)
S2	0.2137(1)	0.1055(4)	0.1428(2)	0.019(1)
S3	0.2108(1)	0.0517(4)	0.8692(2)	0.015(1)
S4	0.1500(1)	0.3838(4)	0.9953(2)	0.022(1)
S5	0.2107(1)	0.8577(4)	0.0948(2)	0.020(1)
S6	0.1403(1)	0.5938(4)	0.2320(2)	0.019(1)
S7	0.1560(1)	0.8477(4)	0.8571(2)	0.016(1)
S8	0.0632(1)	0.8769(4)	0.0645(2)	0.017(1)
S9	0.0645(1)	0.1178(4)	0.1287(2)	0.018(1)
S10	0.0434(1)	0.5852(5)	0.8732(4)	0.035(1)

^a $U_{\text{(eq)}}$ is defined as one-third of the trace of the orthogonalized U_{ij} tensor.

RESULTS AND DISCUSSION

Crystal Structure

The two new quaternary thiophosphates $\text{NaNb}_2\text{PS}_{10}$ and $\text{AgNb}_2\text{PS}_{10}$ are isostructural with a one-dimensional chain framework, where Nb atoms are paired with alternative short and long Nb–Nb interactions. Figure 1a shows the crystal structure of $\text{NaNb}_2\text{PS}_{10}$, which is projected on the *ac*-plane. In Fig. 1b, a side view of one row of the stacked chains of Fig. 1a is shown. It is clear from the figure that cations are filled to make *A*–S (*A* = Na, Ag) contacts near the short Nb–Nb pair and $[\text{PS}_4]$ units, and $[\text{PS}_4]$ units are attached to make bridges between the long Nb–Nb pair. Accordingly, the short and long Nb–Nb interactions depend on whether there is a $[\text{PS}_4]$ unit between the metals or not. The building blocks of

TABLE 5
Atomic Orbital Parameters Used in Extended Hückel Calculations

Atom	Orbital	H_{ii} (eV) ^a	ζ_1	C_1	ζ_2	C_2
S	3s	–20.0	2.122	1.0		
	3p	–13.3	1.827	1.0		
P	3s	–18.6	1.75	1.0		
	3p	–14.0	1.30	1.0		
Nb	5s	–10.1	1.89	1.0		
	5p	–6.86	1.85	1.0		
	4d	–12.1	4.08	0.6401	1.64	0.5516

^a $H_{ii} = \langle \chi_i | H^{\text{eff}} | \chi_i \rangle$, $i = 1, 2, 3, \dots$. The value approximated by valence-state ionization potential.

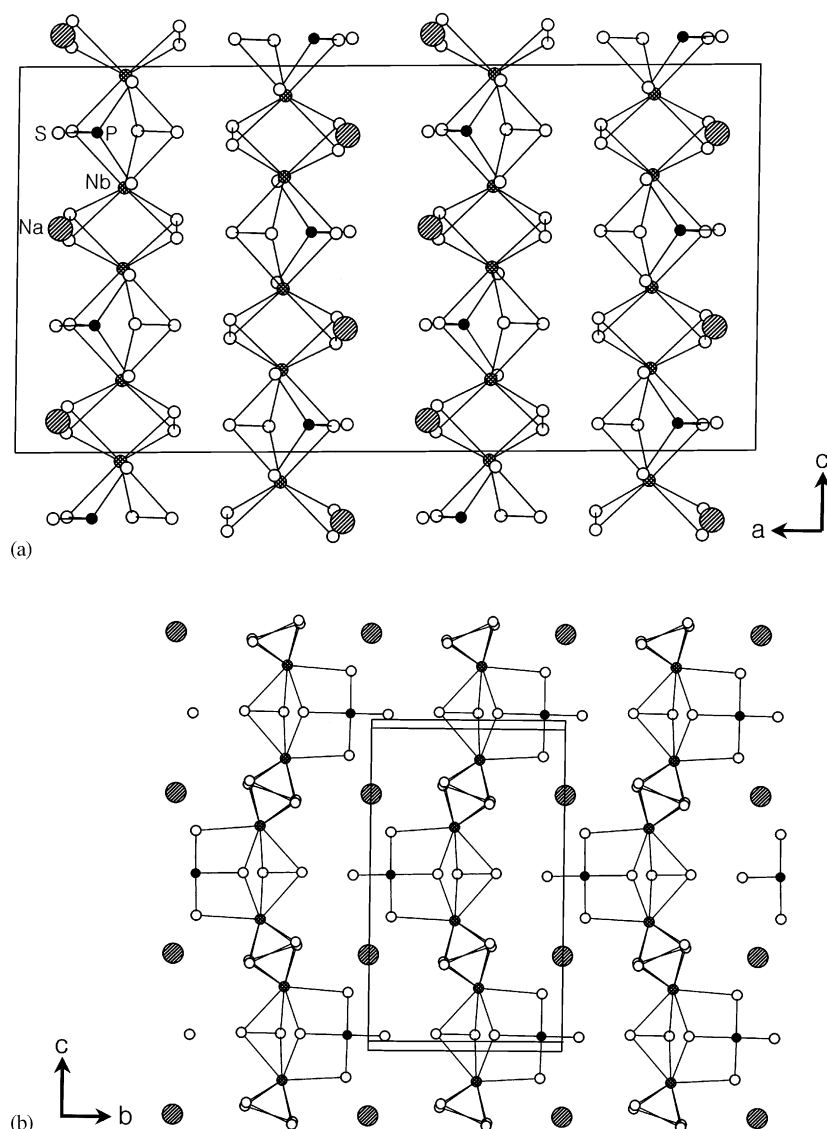


FIG. 1. (a) Crystal structure of NaNb₂PS₁₀ projected along the *b*-axis, where ${}^1_{\infty}[\text{Nb}_2\text{PS}_{10}]$ chains and a unit cell are shown. (b) A side view of one row of the stacked chains in (a). Small open circles are S atoms, small solid circles are P atoms, small cross-shaded circles are Nb atoms, and large shaded circles are Na atoms.

the chains are constructed with [Nb₂S₁₂] and [PS₄] units as shown in Fig. 2. In [Nb₂S₁₂], each Nb atom is centered in a distorted bicapped trigonal prism composed of three S₂²⁻ dumbbells. The bond distances between S and S are in the range of 2.017(2)–2.053(2) Å which is typical for the S₂²⁻ dimer anion. Four sulfur atoms of two S₂²⁻ dumbbells, S(2)–S(5) and S(8)–S(9), form the edges of the trigonal prism. Another two sulfur atoms in the third S₂²⁻ dimer anion, S(3)–S(7), occupy a corner of the prism as well as cap a square face of the trigonal prism. [PS₄] units connect [Nb₂S₁₂] units by sharing the sulfur atoms to form a “biprism chain” ${}^1_{\infty}[\text{Nb}_2\text{PS}_{10}]$. The local symmetry of the building blocks [Nb₂S₁₂] in ANb₂PS₁₀ (*A* = Na, Ag) is

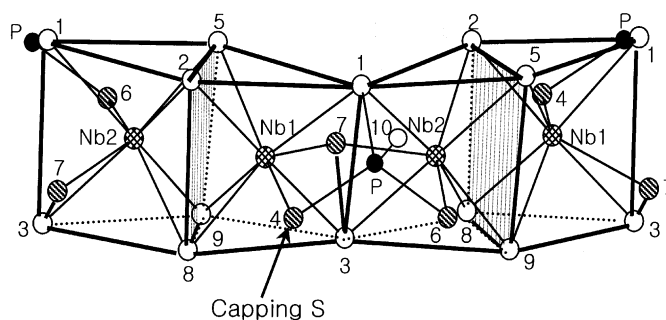


FIG. 2. A side view of “biprism chain” ${}^1_{\infty}[\text{Nb}_2\text{PS}_{10}]$. The [PS₄] units are connected to [Nb₂S₁₂] units by sharing sulfur atoms to form a “biprism chain” ${}^1_{\infty}[\text{Nb}_2\text{PS}_{10}]$. Small cross-shaded circles are Nb atoms, open circles are S atoms forming a trigonal prism, and capping S atoms are shaded.

2-fold rotation symmetry as in $\text{Nb}_4\text{P}_2\text{S}_{21}$ and $\text{KNb}_2\text{PS}_{10}$, while an inversion symmetry is found in $\text{Nb}_2\text{PS}_{10}$.

The overall structures of $A\text{Nb}_2\text{PS}_{10}$ ($A = \text{Na}, \text{Ag}$) are closely related to those of ternary thiophosphates $\text{Nb}_2\text{PS}_{10}$ and $\text{Nb}_4\text{P}_2\text{S}_{21}$ (see Fig. 3). The structures of these two thiophosphates differ in how their biprism chains are linked together by sulfur bridges. $[\text{P}_2\text{S}_8]^{4-}$ units are formed by $-\text{S}-\text{S}-$ bridges in $\text{Nb}_2\text{PS}_{10}$, while $[\text{P}_2\text{S}_9]^{4-}$ units are formed by $-\text{S}-\text{S}-\text{S}-$ bridges between the neighboring chains

in $\text{Nb}_4\text{P}_2\text{S}_{21}$. In $A\text{Nb}_2\text{PS}_{10}$ ($A = \text{Na}, \text{Ag}$), however, instead of having the sulfur bridges between chains, monovalent cations are filled in alternative van der Waals gaps. Therefore, the titled compounds, $A\text{Nb}_2\text{PS}_{10}$ ($A = \text{Na}, \text{Ag}$) can be described as intercalated thiophosphates by alkali metal cations. Recently, the intercalated thiophosphate $\text{KNb}_2\text{PS}_{10}$ was reported by Do and Yun (10); however, its structure is different from those of $A\text{Nb}_2\text{PS}_{10}$ ($A = \text{Na}, \text{Ag}$). For comparison, the structure $\text{KNb}_2\text{PS}_{10}$ is shown in

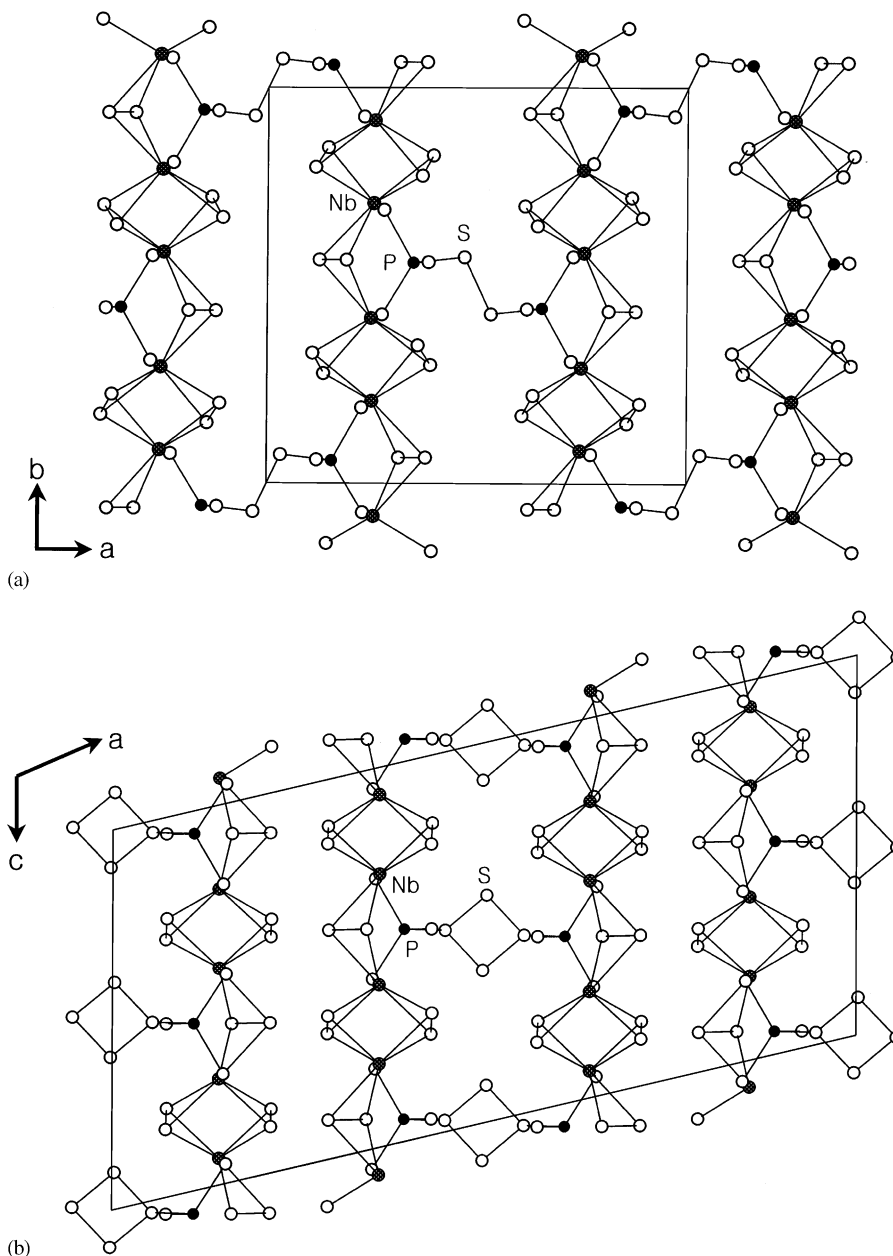


FIG. 3. (a) Crystal structure of $\text{Nb}_2\text{PS}_{10}$. Neighboring chains are bridged by $\text{S}-\text{S}$ bonds. In every chain the direction of the PS_4 unit are alternates. (b) Crystal structure of $\text{Nb}_4\text{P}_2\text{S}_{21}$. Neighboring chains are bridged by $\text{S}-\text{S}-\text{S}$ bonds. In every chain the direction of the PS_4 unit faces the same direction in each chain. Small open circles are S atoms, small solid circles are P atoms, and small cross-shaded circles are Nb atoms.

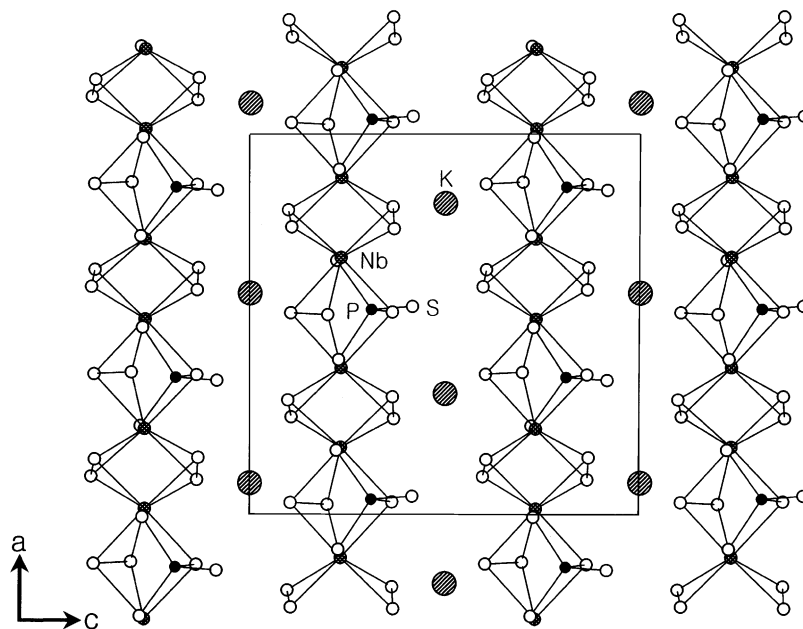


FIG. 4. Crystal structure of $\text{KNb}_2\text{PS}_{10}$ showing $\frac{1}{2}[\text{Nb}_2\text{PS}_{10}]$ chains and unit cells. Small open circles are S atoms, small solid circles are P atoms, small cross-shaded circles are Nb atoms, and large shaded circles are K atoms.

Fig. 4. In $\text{KNb}_2\text{PS}_{10}$, $[\text{PS}_4]$ units are attached between the Nb atoms and directed along the same sides of all chains; therefore, K^+ ions are filled in every gap between rows of the chains around the short Nb–Nb pair. Structurally, each potassium atom can make eight K–S interactions (S atoms in short S–S bonds and in P–S bonds) within the van der Waals distance. On the other hand, the $[\text{PS}_4]$ units are directed alternatively to the opposite sides in $\text{ANb}_2\text{PS}_{10}$ ($A = \text{Na}, \text{Ag}$); thus a zig-zag form is constructed by the $[\text{PS}_4]$ units within the two neighboring chains as in Fig. 1. Cations are filled between the two rows of chains where $[\text{PS}_4]$ units face each other and every other alternate space between the chains remains empty in $\text{NaNb}_2\text{PS}_{10}$ and $\text{AgNb}_2\text{PS}_{10}$. Consequently, the unit cell dimension of $\text{ANb}_2\text{PS}_{10}$ ($A = \text{Na}, \text{Ag}$) along the a -axis direction is doubled compared to the corresponding c -axis of $\text{KNb}_2\text{PS}_{10}$. Although the structures of $\text{NaNb}_2\text{PS}_{10}$ and $\text{AgNb}_2\text{PS}_{10}$ are different from that of $\text{KNb}_2\text{PS}_{10}$, cations reside to make similar A –S ($A = \text{Na}, \text{Ag}$) interactions in each compound. This fact is important to understand how the electron transfer occurs from the K, Na, and Ag atoms to the matrices. Within the given structure, P–S bonds, S–S bonds, and Nb d orbitals can be electron acceptors through K–S, Na–S, or Ag–S interactions.

Table 6 shows the comparisons of the bond distances of $\text{NaNb}_2\text{PS}_{10}$ with other related compounds. The short and long Nb–Nb distances along the chain direction are at 2.891(1) and 3.757(1) Å, respectively, which are similar to the distances found in $\text{KNb}_2\text{PS}_{10}$ and in other ternary compounds $\text{Nb}_2\text{PS}_{10}$ and $\text{Nb}_4\text{P}_2\text{S}_{21}$. The eight Nb–S

distances are in the range of 2.464(2)–2.666(2) Å with an average bond length of 2.550(2) Å in $\text{NaNb}_2\text{PS}_{10}$. The average bond length of P–S bonds is 2.039(3) Å, which is similar to that of $\text{KNb}_2\text{PS}_{10}$.

Electronic Structure

The projected density of states (PDOS) curve calculated for $\text{NaNb}_2\text{PS}_{10}$ is shown in Fig. 5. The PDOS of $\text{AgNb}_2\text{PS}_{10}$ is not shown since it is similar to that of $\text{NaNb}_2\text{PS}_{10}$. The contribution of the sulfur $3p$ orbital to the DOS (see the dotted line in the figure) is mostly found in the occupied region while some part of the orbital at -8 – -7 eV is found in the unoccupied region. It indicates

TABLE 6
Comparisons of Important Bond Distances (Å)
for $\text{ANb}_2\text{PS}_{10}$ ($A = \text{Na}, \text{K}, \text{Ag}$)

Bond distances	$\text{NaNb}_2\text{PS}_{10}$	$\text{KNb}_2\text{PS}_{10}^a$	$\text{AgNb}_2\text{PS}_{10}$	$\text{Nb}_2\text{PS}_{10}^b$	$\text{Nb}_4\text{P}_2\text{S}_{21}^c$
Nb–Nb (Å)	2.891(1)	2.884(2)	2.870(2)	2.869(1)	2.871(1)
	3.757(1)	3.763(2)	3.756(2)	3.766(1)	3.791(1)
P–S (Å) ^d	2.039(3)	2.036(5)	2.039(5)	2.052(4)	2.049(6)
S–S (Å) ^d	2.037(3)	2.040(6)	2.041(5)	2.046(4)	2.041(4)
Nb–S (Å) ^d	2.550(2)	2.541(4)	2.542(3)	2.547(4)	2.552(4)

^a Ref. (10).

^b Ref. (7).

^c Ref. (8).

^d Average distances.

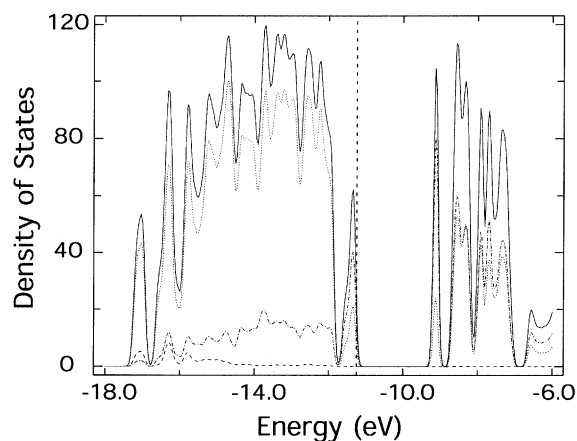


FIG. 5. Projected density of states (PDOS) curve calculated for $\text{NaNb}_2\text{PS}_{10}$. The solid line, the dotted line, the dash-dotted line, and the dashed line represent the total DOS, the PDOS of the S $3p$, the PDOS of the Nb $4d$, and the PDOS of the P $3p$ orbitals, respectively.

that the oxidation state of sulfur is not exactly -2 , but it is slightly higher than -2 . Similarly, strong peak of the Nb d orbital (see the dash-dot line in Fig. 5) is found just below the Fermi energy which means that the oxidation state of Nb is less than $+5$. Upon the results of the PDOS and the valance neutrality, therefore, one can write the oxidation scheme as $(A^+)(\text{Nb}^{4+})_2(\text{S}_2^{2-})_3(\text{PS}_4)^{3-}$ for the $\text{ANb}_2\text{PS}_{10}$ family. Although not shown, molecular orbital calculation on the $(\text{Nb}_4\text{P}_2\text{S}_{20})^{2-}$ unit reveals that the HOMO and LUMO are largely made up of Nb d orbitals. Consequently, Nb d orbitals act as electron acceptors in the $\text{ANb}_2\text{PS}_{10}$ family. This electronic structure is consistent with those found in many transition-metal thiophosphates (11). According to the DOS curve, the compounds turned out to be semiconducting with band gaps of about 1.7 and 1.8 eV for $\text{NaNb}_2\text{PS}_{10}$ and $\text{AgNb}_2\text{PS}_{10}$, respectively, which is consistent with the results of the optical measurement. The results of optical absorption measurement confirm that these compounds are semiconductors with the band gaps of 1.72 and 1.77 eV for $\text{NaNb}_2\text{PS}_{10}$ and $\text{AgNb}_2\text{PS}_{10}$, respectively.

In conclusion, the new quaternary compounds $\text{NaNb}_2\text{PS}_{10}$ and $\text{AgNb}_2\text{PS}_{10}$ were prepared and the structures are characterized. The overall structures of ${}^1_\infty[\text{Nb}_2\text{PS}_{10}^-]$ chains in quaternary compounds $\text{ANb}_2\text{PS}_{10}$ ($A = \text{Na}, \text{Ag}, \text{K}$) are closely related with layered ternary $\text{Nb}_2\text{PS}_{10}$ and $\text{Nb}_4\text{P}_2\text{S}_{21}$. The orientation of a "biprism chain" ${}^1_\infty[\text{Nb}_2\text{PS}_{10}^-]$ of $\text{NaNb}_2\text{PS}_{10}$ and $\text{AgNb}_2\text{PS}_{10}$ is different from that of the already known compound, $\text{KNb}_2\text{PS}_{10}$. Electronic structure calculation shows that the Nb d orbitals possibly become electron acceptors in $\text{ANb}_2\text{PS}_{10}$ ($A = \text{Na}, \text{Ag}, \text{K}$). This conclusion is consistent with the results of Ref. (11). Recently, we obtained $\text{RbNb}_2\text{PS}_{10}$ by reacting alkali metal halide with ternary

$\text{Nb}_4\text{P}_2\text{S}_{21}$. New multinary compounds with various cations will provide better understanding of electrochemical processes of low-dimensional thiophosphates family.

ACKNOWLEDGMENTS

S.-J. Kim acknowledges financial support from the Basic Research Program of the Korean Science & Engineering Foundation (R01-2000-00045). D. Jung acknowledges financial support from the Basic Research Program of the Korea Research Foundation (2000-015-DP0300).

REFERENCES

- (a) A. H. Thompson and M. S. Whittingham, US Patent 4,049,870 (1977) (b) R. Brec and A. Lemehaute, Fr Patenta 7,704,518 and 4,049,879 (1977) (c) Y. Nishi, *Electrochemistry* **68**, 1008 (2000).
- (a) G. Ouvrard, R. Brec, and J. Rouxel, *Mater. Res. Bull.* **20**, 1181 (1985). (b) H. Hahn and W. Klingen, *Naturwissenschaften* **52**, 494 (1965). (c) W. Klingen, G. Eulenberger, and H. Hahn, *Naturwissenschaften* **55**, 229 (1968). (d) R. Brec, G. Ouvrard, A. Louisy, and J. Rouxel, *Ann. Chim-Sci. Mat.* **5**, 499 (1980). (e) B. Taylor, J. Steger, A. Wold, and E. Kostiner, *Inorg. Chem.* **13**, 2719 (1974). (f) M.-H. Whangbo, R. Brec, G. Ouvrard, and J. Rouxel, *Inorg. Chem.* **24**, 2459 (1985). (g) R. Brec, G. Ouvrard, and J. Rouxel, *Mater. Res. Bull.* **20**, 1257 (1985). (h) A. Leautic, E. Riviere, R. Clement, E. Manova, and I. Mitov, *J. Phys. Chem. B* **103**, 4833 (1999).
- (a) S. Lee, *J. Am. Chem. Soc.* **110**, 8000 (1988). (b) J. K. Burdett, S. Lee, and T. J. McLarnan, *J. Am. Chem. Soc.* **107**, 3083 (1985). (c) S. Lee, P. Colombet, G. Ouvrard, and R. Brec, *Inorg. Chem.* **27**, 1291 (1988). (d) S. Lee, R. Colombet, G. Ouvrard, and R. Brec, *Mater. Res. Bull.* **21**, 917 (1986). (e) H. Mutka, C. Payen, P. Molinie, J. L. Soubeyroux, P. Colombet, and A. D. Taylor, *Phys. Rev. Lett.* **67**, 497 (1991). (f) H. Mutka C. Payen, and P. Molinie, *Europhys. Lett.* **21**, 623 (1993).
- R. Brec, G. Ouvrard, M. Evain, P. Grenouilleau, and J. Rouxel, *J. Solid State Chem.* **47**, 174 (1983).
- (a) G. Ouvrard, R. Brec, and J. Rouxel, *Ann. Chim. Fr.* **7**, 53 (1982). (b) R. Brec, G. Ouvrard, R. Freour, J. Rouxel, and J. L. Soubeyroux, *Ann. Chim-Sci. Mat.* **18**, 689 (1983).
- M. Evain, R. Brec, G. Ouvrard, and J. Rouxel, *J. Solid State Chem.* **56**, 12 (1985).
- R. Brec, P. Grenouilleau, M. Evain, and J. Rouxel, *Rev. Chim. Miner.* **20**, 295 (1983).
- R. Brec, M. Evain, P. Grenouilleau, and J. Rouxel, *Rev. Chim. Miner.* **20**, 283 (1983).
- P. Grenouilleau, R. Brec, M. Evain, and J. Rouxel, *Rev. Chim. Miner.* **20**, 628 (1983).
- J. Do and H. Yun, *Inorg. Chem.* **35**, 3729 (1996).
- M. Evain, R. Brec, and M.-H. Whangbo, *J. Solid State Chem.* **71**, 244 (1987).
- G. M. Sheldrick, *Acta Crystallogr. A* **46**, 467 (1990).
- G. M. Sheldrick, "SHELXL 93, Program for the Refinement of Crystal Structures," University of Göttingen, 1993.
- (a) R. Hoffmann, *J. Chem. Phys.* **39**, 1397 (1963). (b) J. Ren, W. Liang, and M.-H. Whangbo, CAESAR, Primecolor Software, Inc., Cary, NC, 1999.
- G. Kortüm, "Reflectance Spectroscopy," Springer-Verlag, New York, 1969.